

Bayesian Hypothesis Testing for Planet Detection

Isabelle Braems¹

Laboratoire d'Etudes des Matriaux Hors-Equilibre (LEMHE)

N. Jeremy Kasdin

Princeton University

ABSTRACT

The past five years has seen a surge in research and innovative ideas for the imaging of extrasolar planets, particular terrestrial ones. We expect that within the next decade a space observatory will be launched with the objective of imaging earthlike planets. Because of the limited lifetime of such a mission and the large number of potential targets, integration time is a critical parameter. In fact, integration time is the primary metric in evaluating various design approaches for the high contrast imaging system. In this paper we present a new approach to determining the existence of a planet in an observed system using Bayesian hypothesis testing. Rather than perform photometry, or rely on vision to determine the existence of a planet, this approach evaluates the image plane data statistically under certain assumptions about the prior probability distributions. We show that extremely high confidence can be achieved in substantially shorter integration times than conventional photometric methods.

1. Introduction

The discovery of more than 100 extrasolar Jupiter-sized planets in just the last decade has generated enormous interest, both among astronomers and the public, in the problem of discovering and characterizing Earthlike planets. NASA is already planning its next large space-based observatory, the *Terrestrial Planet Finder (TPF)*, with a planned launch date toward the end of the next decade. TPF's primary objective will be to discover Earthlike planets and characterize them for indications of life.

The technical challenges for TPF are great. Foremost among them is the problem of high-contrast imaging. In order to discover as many planets as possible, it is necessary to design an imaging systems that achieves very high contrast between the parent star and the planet as close as possible to the star. An earlier study by Brown et al. (2002) indicates that a $D = 4\text{m}$ class visible-light (i.e. $400\text{nm} \leq \lambda \leq 650\text{nm}$) instrument ought to be able to discover about 50 extrasolar Earth-like planets if it can provide contrast of 10^{-10} at an angular separation of $3\lambda/D$ and that a $4 \times 10\text{m}$ class telescope ought to be able to discover about 150 such planets if it can provide the same contrast at a separation of $4\lambda/D$.

¹I. Braems received a fellowship from the Institut National de Recherche en Informatique et Automatique (INRIA)

There are myriad of methods being proposed to achieve the high contrast necessary for planet detection. Our interest has been in shaped pupil coronagraphy. Many of our optimal approaches are described in Kasdin et al. (2003); Vanderbei et al. (2003a,b). Of particular importance is the discussion in Kasdin et al. (2003) on performance metrics used to compare and optimize various coronagraphic approaches. The key factor here is integration time. All planet finding missions must minimize the integration time in order to provide the most possible observations and the least sensitivity to instabilities in the telescope and spacecraft. To that end, quantitative measures of integration time, derived for specific image processing techniques, are essential.

In Kasdin et al. (2003) we discussed a number of different approaches for planet detection, each with a corresponding integration time to reach a specified signal-to-noise ratio (S/N). The objective was to find quantitative metrics that could be used to compare different coronagraph approaches. The simplest detection integration time threshold, t_1 , was proposed such that for $\tau \geq t_1$ the decision of whether a planet exists can be taken by a human eye. This threshold is based on the expected signal to noise ratio S/N

$$S/N = \frac{I_p \Delta P}{\sqrt{I_b \Delta S}} \sqrt{t_1}, \quad (1)$$

where it is assumed that the planet intensity I_p is known, the background is uniform and its intensity I_b is also known and ΔP is the area under the PSF P in the integration area ΔS around the planet location to be denoted ζ^* , where ζ^* refers to the (continuous) location in the image plane of the central peak of the planet's PSF (note that ζ^* can be considered a member of \mathbb{R}^2 , thus representing the two-dimensional position of the planet on the image plane). The usual assumption is that the human eye can detect a planet when the S/N ratio exceeds 5, setting the typical detection criterion. Note the dependence on PSF shape; as the coronagraphs we are considering operate by modifying the shape of the PSF, there is some sensitivity of the integration time to the specific coronagraph design. Brown and Burrows (1990) call this ratio of PSF area to pixel area the “sharpness”.

Unfortunately, this photometric approach to detection is limited, as it relies on an empirical criterion that does not provide any information about the confidence level to be associated with the collected images. In Kasdin et al. (2003), other integration times were computed but they were based on the assumption that photometry was performed on the image in an effort to estimate the planet (and perhaps background) irradiance. The goal of this paper is to establish a simple detection criterion to be used before any photometry analysis in order to allow a smaller integration time, while providing quantitative information on the confidence associated with a planet decision. We also plan to study modifications of the coronagraph design optimization using these results.

The basic principle is to use probabilistic hypothesis testing to confirm or deny the hypothesis that a planet is located at a given pixel. Among several hypothesis testing techniques, Bayesian approaches seem promising. Their appeal stems, in large part, from the fact that these tests are conditioned on the collected data, no matter the amount, while *frequentist* approaches require interpolation on fictitious data (as multiple data sets for determining statistics will not be available). Moreover, the mathematical framework of Bayesian methods includes marginalization, *i.e.*, an easy way to take into account uncertain nuisance parameters (see Berger (1985)). For these reasons and others, Bayesian techniques have resulted in a significant breakthrough

in the last decade (see for example Loredo (1992), Gregory and Loredo (1992), Defay et al. (2001) and Aigrain and Favata (2002)).

For the sake of simplicity and demonstration, we only consider 1D images in this work (that is, the dependence of the PSF along only one axis of the image plane). While the real image is a continuous function of the position ζ : $\mathcal{F}(\zeta) = I_b + I_p P(\zeta - \zeta^*)$, the CCD collects a photon noise corrupted discretized image $Z = (z_n)_{n=1,\dots,M}$ where z_n stands for the intensity of the n -th pixel. We use n^* to indicate the index of the pixel containing ζ^* : $\zeta^* \in [n^* \Delta\alpha, (n^* + 1) \Delta\alpha]$. Due to the low photon count at these short integration times, each z_n is modeled as a Poisson random variable whose mean is

$$\lambda_n(I_b, I_p, \zeta^*) = \tau \left(I_b \Delta\alpha + I_p \int_{\zeta_n}^{\zeta_{n+1}} P(\zeta - \zeta^*) d\zeta \right) \triangleq \tau(I_b \Delta\alpha + I_p \Delta P_n(\zeta^*)), \forall n = 1, \dots, M. \quad (2)$$

where $\Delta\alpha$ is the size of a pixel and (ζ_n, ζ_{n+1}) refer to the location of the edges of pixel n . In this preliminary study, we will assume that I_b is uniform, we will neglect the speckle noise due to imperfect optics, and we will consider only monochromatic signals. Clearly these are rather restrictive assumptions, but they allow us to focus attention on the technique and compare our results to the previous one. We hope during the next few years to expand this effort and use the same Bayesian ideas on the more realistic polychromatic system with speckle. For instance, a planet might be separated from speckle by incorporating into the model a few discrete frequencies (most likely via a dichroic) or via multiple measurements at different observatory orientations.

2. Detection criterion

In most cases (except Gregory and Loredo (1992)) Bayesian approaches were used only to solve the inverse problem of denoising the collected image. This would correspond to estimating I_p (i.e., it corresponds to the photometric approaches proposed in Kasdin et al. (2003)) or to estimating ζ^* (the localization problem) from Eq. 2. Both of these approaches by necessity already assume that a planet is present and typically take more time. A hypothesis testing approach is a direct approach that will more appropriately be performed before any further processing.

2.1. Odds ratio

As the objective is not only to detect a potential planet but also its discrete location n^* , we propose a test to be performed on each pixel. To determine whether a potential planet is present in the n -th pixel, we compare the probabilities of the following two alternate hypotheses:

$$\begin{aligned} H_0^n &: \text{there is no planet in the } n\text{-th pixel,} \\ H_1^n &: \text{there is a planet in the } n\text{-th pixel.} \end{aligned}$$

Associate a model M_i to each hypothesis H_i :

$$\begin{aligned} M_0^n &: \lambda_n = \lambda_n(I_b, I_p, \zeta^*), \quad \zeta^* \in [n\Delta\alpha, (n+1)\Delta\alpha], \quad I_p = 0 \\ M_1^n &: \lambda_n = \lambda_n(I_b, I_p, \zeta^*), \quad \zeta^* \in [n\Delta\alpha, (n+1)\Delta\alpha], \quad I_p \neq 0 \end{aligned}$$

We now compare the posterior probabilities of the two models conditioned on the collected data, and we shall decide that there is a planet in pixel n if the *odds ratio*, O_{10}^n , favors H_1^n over H_0^n :

$$O_{10}^n = \frac{p(M_1^n|Z)}{p(M_0^n|Z)} = \frac{p(M_1^n)p(Z|M_1^n)}{p(M_0^n)p(Z|M_0^n)} \quad (3)$$

where we have used Bayes' rule to write the odds ratio as the product of the ratio of prior probabilities $\frac{p(M_1^n)}{p(M_0^n)}$ and the ratio of likelihoods $\frac{p(Z|M_1^n)}{p(Z|M_0^n)}$. This dependence on the prior probability of a terrestrial planet in a given system (often referred to as η_{Earth}) is one of the most attractive features of the Bayesian approach, as information from prior missions such as Kepler can be explicitly included in the detection algorithm and the sensitivity of the detection to these assumptions can be quantitatively assessed.

One possible decision criterion would be that $O_{10}^n > 1$ favors H_1^n , thus indicating that there is a planet whose true location ζ^* is inside the n -th pixel. Alternatively, the decision can be made based on a different value of the ratio derived from particular weighting criteria. We call this a “Loss-based decision” and describe it next.

2.2. Loss-based decision

As mentioned above, a decision criterion based on an odds ratio of unity is not the only possible one. In particular, an alternative criteria uses a weighted decision based upon our sensitivity to different types of errors (for instance, we may be more willing to tolerate missed detections than false alarms). To quantify this we define two possible actions:

$$a_0 : \text{“we accept } H_0 \text{”} \quad a_1 : \text{“we reject } H_0 \text{”}.$$

The Receiving Operator Curve (ROC) is used to determine the best possible decision threshold and quantify the relative importance of the two types of errors. The ROC is a plot of the evolution of the missed detection probability (Type II error), $p(a_0|H_1^n)$, versus $1 - p(a_1|H_0^n)$, where $p(a_1|H_0^n)$ is the false alarm rate (Type I error). In other words, we place a point on the curve corresponding to the two probabilities for every possible threshold value, from 0 to infinity. We then typically select the threshold corresponding to the “knee” of the curve, that is, the combination of maximum probability of success with minimum likelihood of missed detection. The area under the ROC is defined as the “power” of the test and for the results below is parameterized by the integration time. A perfect test is one with zero probability of missed detection and zero probability of false alarm, resulting in a power value (area under the ROC) of one. The values of the

probabilities for the curve are found through Monte Carlo simulations.²

2.3. Likelihoods and priors

To compute O_{10}^n as defined in Eq. 3, we need to assign the priors $p(M_i^n)$, $i = 1, 2$ and compute the likelihoods $p(Z|M_i^n)$, $i = 1, 2$. In the absence of any other information, we assume here that the two models are *a priori* equiprobable at each pixel: $p(M_0^n) = \frac{1}{2}$, $p(M_1^n) = \frac{1}{2}$, $\forall n = 1, \dots, M$.

In general, the probability of a given data set depends on various physical parameters of the system. For instance, the mean photon rate in the Poisson distribution depends on the irradiance and the planet location in the pixel. In order to compute the likelihood, we must *marginalize* the probability to remove this parameter dependence. The marginalization law allows us to compute the global likelihood of the model $M_i^n(\psi)$ over its parameter vector denoted by ψ :

$$p(Z|M_i^n) = \int d\psi p(\psi|M_i^n) p(Z|\psi, M_i^n). \quad (4)$$

Modeling each pixel intensity z_j as an independent Poisson random variable, we obtain

$$p(Z|\psi, M_i^n) = \prod_{j=1}^M p(z_j|\psi, M_i^n) = \prod_{j=1}^M \frac{\lambda(\psi, M_i^n)_j^{z_j}}{z_j!} \exp(-\lambda(\psi, M_i^n)_j) \quad (5)$$

which we multiply by the prior probabilities and then integrate over ψ to determine the likelihoods as in Eq. 4.

To determine the prior probabilities, we assume that all the parameters are independent, resulting in:

$$p(I_p, I_b, \zeta^*|M_1^n) = p(I_p|M_1^n) p(I_b|M_1^n) p(\zeta^*|M_1^n),$$

where here ψ consists of the planet and background irradiances and the planet location. We thus need to assign prior probabilities to each parameter individually. The choice of specific densities for the priors is a delicate subject as there is not necessarily a sound theoretical basis for the choice and particular priors may effect the performance of the estimator. Our approach here is to make a sensible choice for the priors that also makes the mathematical analysis manageable. In future work we will examine the effect on the probability of success when the assumed prior densities are actually in error.

The continuous planet location ζ^* is assumed to be uniform over a pixel containing a planet:

$$\begin{aligned} p(\zeta^*|M_1^n) &= \frac{1}{\Delta\alpha} \quad \text{when } \zeta^* \in [n\Delta\alpha, (n+1)\Delta\alpha], \\ &= 0 \quad \text{otherwise.} \end{aligned}$$

²It was found empirically that the optimal threshold value strongly depends upon the shape of the PSF, with a unity threshold best only for a square PSF.

As the intensity I_p of the planet is strictly positive, it has been modeled by a Gamma law $\Gamma(\alpha, \beta)$ of mean $E[I_p] = \alpha\beta$ and variance $E[I_p^2] = \alpha\beta^2$. A second advantage of this model is that the gamma distribution is the conjugate prior of a Poisson law (Berger (1985)), thus simplifying future computations:

$$p(I_p | M_1^n) = I_p^{\alpha-1} \exp\left(-\frac{I_p}{\beta}\right). \quad (6)$$

We will either assume that the intensity of the background I_b is known or that it also follows a Gamma law, $\Gamma(a, b)$.

3. Results

For simplicity, all the results provided in this section have been performed for a 1-D point spread function, that is, a cross section of the two-dimensional image. This function for optimal shaped pupil coronagraphs is the transform of the prolate spheroidal wavefunction (see Kasdin et al. (2003) or Vanderbei et al. (2003a)). In future work we will repeat and compare to a number of different pupil designs (as well as other types of coronagraphs) and extend to two-dimensions. All results are based on Monte-Carlo simulations.

To account for the size of the PSF, which extends over more than one pixel, we define Δ as the width of the significant part of the PSF (normally taken equal to the FWHM), and set

$$K = \text{ceil}\left(\frac{\Delta}{\Delta\alpha}\right)$$

such that $2K + 1$ is the maximum number of pixels that can be covered by the truncated PSF and $\Delta S = (2K + 1)\Delta\alpha$. For a pixel n_j such that $\|n_j - n\| > K$, $\lambda(\psi, M_0^n)_j = \lambda(\psi, M_1^n)_j = I_b\Delta\alpha\tau$. The ratio of likelihoods as defined in Eq. 5 only involves the pixels covered by Δ :

$$\begin{aligned} \frac{p(Z|\psi, M_1^n)}{p(Z|\psi, M_0^n)} &= \frac{\prod_{j=1}^M p(z_j|\psi, M_1^n)}{\prod_{j=1}^M p(z_j|\psi, M_0^n)} \\ &= \prod_{j=\max(n-K, 1)}^{\min(n+K, M)} \frac{p(z_j|\psi, M_1^n)}{p(z_j|\psi, M_0^n)} \\ &= \prod_{j=\max(n-K, 1)}^{\min(n+K, M)} \left(\frac{\lambda(\psi, M_1^n)_j}{\lambda(\psi, M_0^n)_j} \right)^{z_j} \exp -(\lambda(\psi, M_1^n)_j - \lambda(\psi, M_0^n)_j) \end{aligned}$$

where M is the total number of pixels.

In the following simulations we have selected the pixel size such that $K = 2$, and for the sake of simplicity, we will consider n such that $\max(n - K, 1) = n - K$, $\min(n + K, M) = n + K$ (no edge).

3.1. Assume I_p and I_b are known

For this study, we use Monte-Carlo simulations to determine the effectiveness of the hypothesis testing criterion and the resulting probabilities of type I and II errors for a given normalized integration time, τ . This can then be compared to the decision criterion described in Kasdin et al. (2003) and based on Eq. 1 for $t_1 = \tau$. In this section, the simulations assume I_p and I_b are both known. In reality, of course, not only is I_p not necessarily known, it varies with pixel location as the planet moves further away from the star (assuming a reflected visible light system). This assumption is relaxed in later sections.

Under these assumptions, the odds ratio in favor of H_1^n is (see Appendix):

$$O_{10}^n = \frac{1}{\Delta\alpha} \exp(-\tau I_p \Delta P) \int_0^{\Delta\alpha} \prod_{j=n-K}^{j=n+K} \left(1 + \frac{Q}{\Delta\alpha} \Delta P_j(\theta)\right)^{z_j} d\theta, \quad (7)$$

where $Q = \frac{I_p}{I_b}$ and $\Delta P_j(\theta)$ is the area of the PSF covered by one of the five pixels (indexed by j) when the planet appears at location θ in pixel n . Figure 1 depicts the results obtained for two simulated sets of images. For $i \in [1, 500]$, the data are simulated without any planet ($Q = 0$), while for $i \in [501, 1000]$, $Q = 1$, the planet is located in pixel $n^* = 11$. For all simulations, the normalized integration time was set to $\tau = 1$, corresponding to a signal-to-noise ratio S/N computed as in Eq. 1 of 3.52. While it is reasonable to expect some detections using the conventional approach with this S/N ratio, using the usual criteria of $S/N = 5$ described above, no planets would be detected. Figure 2 depicts the histogram of $\log O_{10}^{n^*}$ for the two simulated sets. For a threshold equal to one, the false alarm rate is 0.1%, while the missed detection rate reaches 7.2%. From the ROC curve (not plotted here for brevity), we determined that the test has maximal power if the threshold is set to 0.158 rather than 1. With this threshold, the false alarm rate is 4.0% and the missed detection rate is 3.0%. This demonstrates that under the same assumptions, the Bayesian technique is extremely effective at detection with quantifiable performance and at shorter integration times.

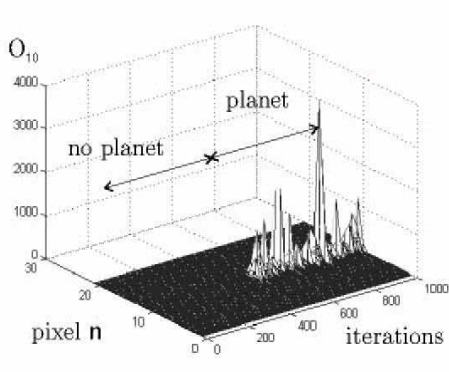


Fig. 1.— Value of O_{10}^n as a function of n for the two simulated sets, for $\tau = 1$.

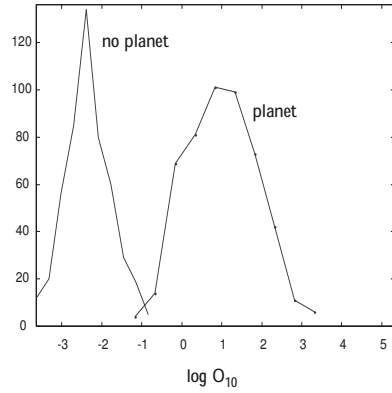


Fig. 2.— Histogram of $\log O_{10}^{n^*}$ for the two simulated sets, $\tau = 1$

3.2. Assume I_p is uncertain

The first complication to consider is a lack of knowledge of I_p . In Kasdin et al. (2003), we take the approach of estimating I_p (whether a planet is there or not) and examining the quality of the estimate to make the decision. Here, we avoid photometry and still use a Bayesian hypothesis testing approach to make the decision in a shorter integration time.

If we assume under H_1 that I_p follows a gamma law, $\Gamma(\alpha, \beta)$, then using Eqs. 3 and 4 we get

$$O_{10}^n = \frac{1}{\Delta\alpha} \sum_{p=0}^{p=\sum_{j=n-K}^{n+K} z_j} \frac{\Gamma(\alpha + p)}{\Gamma(\alpha)} \left(\frac{\beta}{I_b}\right)^p \frac{1}{(1 + \tau\beta\Delta P)^{\alpha+p}} \int_0^{\Delta\alpha} \gamma_p(\theta) d\theta \quad (8)$$

where the coefficients $\gamma_p(\theta)$ are provided in the Appendix. The data have been simulated for $\tau = 1$, with $\alpha = 4$ and $\beta = QI_b/4$. The histogram of the resulting estimated S/N using Eq. 1 and the I_p selected from the distribution from each run is depicted on Figure 3. Following Eq. 1, if a conclusion is reached only for $S/N > 5$, the missed detection rate reaches 72.7%. As described in Section 3.1, the mean value of I_p was chosen to correspond to a S/N of 3.52 for $\tau = 1$. When I_p is sampled from the gamma distribution here (with the same mean value), roughly 24% of the time a planet occurs with a mean $S/N > 5$ that would assure a detection by the conventional approach. For the same simulated data, our criterion provides a missed detection rate of only 1.0% with the odds ratio decision threshold set at one.

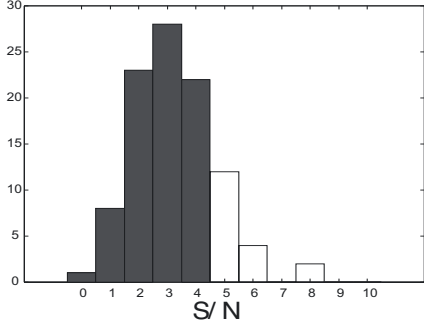


Fig. 3.— Histograms of the estimated S/N when the planet intensity I_p follows a Gamma law. The blue boxes correspond to the case where $S/N < 5$, *i.e.* that an existing planet has not been detected.

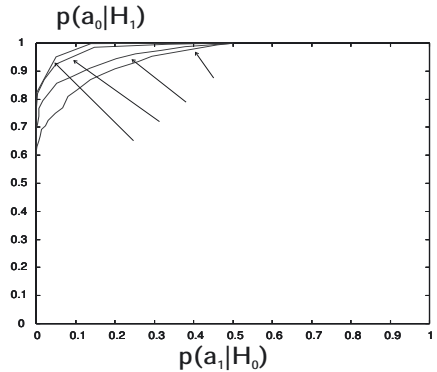


Fig. 4.— ROC curves as a function of the relative integration time τ : the power of the test increases with τ

The Receiver Operating Curves for this case is depicted in Figure 4. It shows the trade-off between the false alarm and the missed detection rates for different values of the relative integration time τ . As expected, the greater τ , the more powerful the test. Nevertheless, note that a relatively high correct decision probability $p(a_0|H_0) + p(a_1|H_1)$ (found via the Monte Carlo results with a decision threshold of one) can

be achieved even for low integration times (see Table 1). In practice on real data we may choose the lower optimal threshold deduced from the simulations, thus achieving slightly higher probabilities of success.

τ	0.1	0.2	0.5	1
$p(a_0 H_0) + p(a_1 H_1)$	0.732	0.804	0.876	0.900

Table 1: Evolution of the correct decision probability with τ

3.3. Assume I_b is also unknown

The final, and most complicated, case is to assume that both I_p and I_b are unknown. Again, in our previous report and in Kasdin et al. (2003), we resorted to two-parameter least-squares estimation (matched filtering) on the photometric data. By simultaneously estimating the irradiance of the planet and the background, a decision can be made on the planet, but the integration times become quite long. With the Bayesian approach, we found that we have a very high probability of success even at the same integration time as the previous case.

For the sake of brevity, we defer the derivation to the Appendix. If $p(I_b) = \Gamma(a, b)$, we use the marginalization law Eq. 4 to eliminate its dependence from the odds ratio and obtain:

$$O_{10}^n = \frac{1}{\Delta\alpha} \frac{1}{(1 + \beta\tau\Delta P)^{\alpha+p}} \sum_{p=0}^{p=\sum_{j=n-K}^{n+K} z_j} \frac{\Gamma(\alpha+p)}{\Gamma(\alpha)} \left(\frac{\beta'}{b'}\right)^p \frac{\Gamma(\sigma_K - p)}{\Gamma(\sigma_K + a)} \int_0^{\Delta\alpha} \gamma_p(\theta) d\theta$$

where

$$\frac{1}{b'} = \frac{1}{b} + \tau\Delta S$$

A similar Monte-Carlo study as before shows that we can reach a correct decision probability of 0.84 for the same integration time ($\tau = 1$) with $\frac{E[I_p]}{E[I_b]} = 1$ and $E[I_p^2] = E[I_b]/2$, $E[I_b^2] = E[I_b]/2$.

4. Conclusion

Bayesian hypothesis testing is a promising approach to planet detection and to associate a quantitative confidence level with the detection system, with a relative integration time smaller than t_1 and without performing photometry. Moreover this approach allows us to take into account the uncertainty associated with the nuisance parameters such as the intensity of the background via the marginalization law. Nevertheless, choosing a prior may strongly influence the quality of the result. Further work aims to develop this same approach with other priors and to study its robustness.

No speckle has been considered yet. Current work aims at defining a three-hypothesis test to detect if the pixel under study contains a planet, speckle, or just noise. A trio of three bandpass filters, while allowing us to consider quasi-monochromatic signals (and directly applying this technique), would also permit us to

define speckle as a space-variant component. Note that adding other features in addition to just the PSF shape in a Bayesian or optimal classifier could also improve the results.

REFERENCES

R. A. Brown, C. J. Burrows, S. Casertano, M. Clampin, D. Eggetts, E.B. Ford, K.W. Jucks, N. J. Kasdin, S. Kilstrom, M. J. Kuchner, S. Seager, A. Sozzetti, D. N. Spergel, W. A. Traub, J. T. Trauger, and E. L. Turner. The 4-meter space telescope for investigating extrasolar earth-like planets in starlight: TPF is HST2. In *Proceedings of SPIE: Astronomical Telescopes and Instrumentation*, number 14 in 4860, 2002.

N. J. Kasdin, R. J. Vanderbei, D. N. Spergel, and M. G. Littman. Extrasolar planet finding via optimal apodized-pupil and shaped-pupil coronagraphs. *The Astrophysical Journal*, 582:1147–1161, January 2003.

R.J. Vanderbei, D.N. Spergel, and N.J. Kasdin. Spiderweb Masks for High Contrast Imaging. *Astrophysical Journal*, 590:593–603, June 10 2003a.

R.J. Vanderbei, D.N. Spergel, and N.J. Kasdin. Circularly Symmetric Apodization via Starshaped Masks. *Astrophysical Journal*, 599(1):686–694, December 10 2003b.

R. A. Brown and C. J. Burrows. On the feasibility of detecting extrasolar planets by reflected starlight using the hubble space telescope. *Icarus*, 87:484–497, 1990.

J. Berger. *Statistical decision theory and Bayesian analysis*. Springer-Verlag, 1985.

T. Loredo. The promise of bayesian inference for astrophysics. In *Statistical Challenges in Modern Astronomy*, pages 275–297. Springer-Verlag, 1992.

P. Gregory and T. Loredo. A new method for the detection of a periodic signal of unknown shape and period. *The Astrophysical Journal*, 298:146–168, 1992.

C. Defay, M. Deleuil, and P. Barge. A bayesian method for the detection of planetary transits. *Astronomy and Astrophysics*, 365(2):330–340, 2001.

S. Aigrain and F. Favata. Bayesian detection of planetary transits: a modified version of the gregory-loredo method for bayesian periodic signal detection. *Astronomy and Astrophysics*, 395:625–636, 2002.

A. Appendix

A.1. PSF Truncation

Let Δ be the FWHM of the PSF. The maximum number of pixels that can be covered by the PSF is an even number denoted by $2K + 1$ where

$$K = \text{ceil} \left(\frac{\Delta}{\Delta\alpha} \right).$$

As

$$p(z_k|M_1^n) = p(z_k|M_0), k \notin [n-K, n+K]$$

Then

$$O_{10}^n = \frac{\prod_{k=1}^M p(z_k|M_1^n)}{\prod_{k=1}^M p(z_k|M_0^n)} = \frac{\prod_{k=n-K}^{n+K} p(z_k|M_1^n)}{\prod_{k=n-K}^{n+K} p(z_k|M_0^n)} \triangleq \frac{L_1(I_p, I_b, \theta)}{L_0(I_b)}$$

Example. If $K = 1$, 3 pixels only can be involved,

$$O_{10}^n = \frac{p(z_{n-1}|M_1^n) p(z_n|M_1^n) p(z_{n+1}|M_1^n)}{p(z_{n-1}|M_0^n) p(z_n|M_0^n) p(z_{n+1}|M_0^n)}$$

In the following, we will use the following notation

$$\sigma_K \triangleq \sum_{k=n-K}^{n+K} z_k; \pi_k \triangleq \prod_{k=n-K}^{n+K} z_k!$$

A.2. I_p is assumed to be known

Obviously, as I_b is assumed to be known

$$p(Z|M_0^n) = \int_{\mathbb{R}} p(Z|M_0^n, I_b) p(I_b) dI_b = p(Z|M_0^n, I_b).$$

For the constant-rate model M_0^n

$$\begin{aligned} L_0(I_b) &= \prod_{k=n-K}^{n+K} p(z_k|M_0^n, I_b) = \prod_{k=n-K}^{n+K} \frac{1}{z_k!} \lambda_k^{z_k} \exp(-\lambda_k) \\ &= \prod_{k=n-K}^{n+K} \frac{1}{z_k!} (I_b \Delta \alpha \tau)^{z_k} \exp(-I_b \Delta \alpha \tau) = \frac{1}{\pi_K} (I_b \tau \Delta \alpha)^{\sigma_K} \exp(-I_b \tau \Delta S), \end{aligned}$$

where $\Delta S = (2K + 1) \Delta \alpha$ is the area of integration around the $n'th$ pixel.

Assuming that θ is uniform on $[\zeta_n, \zeta_{n+1}]$, the likelihood of the alternative model M_1^n is

$$\begin{aligned} L_1(I_p, I_b) &= \int_{\zeta_n}^{\zeta_{n+1}} p(Z|M_1^n, I_b, I_p, \theta) p(\theta) d\theta \\ &= \frac{1}{\Delta \alpha} \int_{\zeta_n}^{\zeta_{n+1}} d\theta \prod_{k=n-K}^{n+K} p(z_k|M_1^n, I_b, I_p, \theta) \\ &= \frac{1}{\Delta \alpha} \int_{\zeta_n}^{\zeta_{n+1}} d\theta \frac{1}{\pi_K} \prod_{k=n-K}^{n+K} (I_b \Delta \alpha \tau + I_p \Delta P_k(\theta))^{z_k} \exp(-\tau(I_b \Delta \alpha + I_p \Delta P_k(\theta))) \end{aligned}$$

Compute

$$\begin{aligned} A_1(\theta) &= \prod_{k=n-K}^{n+K} (I_b \Delta \alpha \tau + \tau I_p \Delta P_k(\theta))^{z_k} \exp(-\tau(I_b \Delta \alpha + I_p \Delta P_k(\theta))) \\ &= (I_b \tau \Delta \alpha)^{\sigma_K} \exp(-I_b \tau \Delta S) \prod_{k=n-K}^{n+K} \left(1 + \frac{I_p \Delta P_k(\theta)}{I_b \tau \Delta \alpha}\right)^{z_k} \exp\left(-\tau \sum_{k=n-K}^{n+K} I_p \Delta P_k(\theta)\right) \\ &= (I_b \tau \Delta \alpha)^{\sigma_K} \exp(-\tau(I_b \Delta S + I_p \Delta P)) \prod_{k=n-K}^{n+K} \left(1 + Q \frac{\Delta P_k(\theta)}{\Delta \alpha}\right)^{z_k} \end{aligned}$$

by noting that $\sum_{k=n-K}^{n+K} \Delta P_k(\theta) = \Delta P$ and by noting $Q = \frac{I_p}{I_b}$. We then have

$$L_1(I_p, I_b) = \frac{(I_b \tau \Delta \alpha)^{\sigma_K}}{\Delta \alpha \pi_K} \exp(-\tau(I_b \Delta S + I_p \Delta P)) \int_{\zeta_n}^{\zeta_{n+1}} d\theta \prod_{k=n-K}^{n+K} \left(1 + Q \frac{\Delta P_k(\theta)}{\Delta \alpha}\right)^{z_k}$$

$$\begin{aligned} O_{10}^n(I_p, I_b) &= \frac{L_1(I_p, I_b)}{L_0(I_b)} \\ &= \frac{1}{\Delta \alpha} \exp(-\tau I_p \Delta P) \int_{\zeta_n}^{\zeta_{n+1}} d\theta \prod_{k=n-K}^{n+K} \left(1 + Q \frac{\Delta P_k(\theta)}{\Delta \alpha}\right)^{z_k} \end{aligned}$$

A.3. Assume I_p is uncertain

As I_b is still assumed to be known, L_0 is unchanged. Using the marginalization law, we have

$$\begin{aligned} O_{10}^n(I_b) &= \frac{\int_0^\infty p(I_p) L_1(I_p) dI_p}{L_0(I_b)} \\ &= \frac{1}{\Delta\alpha} \int dI_p p(I_p) \exp(-\tau I_p \Delta P) \int_{\zeta_n}^{\zeta_{n+1}} d\theta \prod_{k=n-K}^{n+K} \left(1 + \frac{I_p}{I_b} \frac{\Delta P_k(\theta)}{\Delta\alpha}\right)^{z_k} \\ &= \frac{1}{\Delta\alpha \Gamma(\alpha) \beta^\alpha} \int_{\zeta_n}^{\zeta_{n+1}} d\theta \int_0^\infty dI_p I_p^{\alpha-1} \exp\left(-\frac{I_p}{\beta'}\right) \prod_{k=n-K}^{n+K} \left(1 + I_p \frac{\Delta P_k(\theta)}{I_b \Delta\alpha}\right)^{z_k}, \end{aligned}$$

by posing

$$\frac{1}{\beta'} = \frac{1}{\beta} + \tau \Delta P$$

For the sake of simplicity, we only present here the case for $K = 2$ (case described in the main document).

Using the binomial law

$$(1 + \alpha x)^\beta = \sum_{n=0}^{\beta} \binom{\beta}{n} \alpha^n x^n$$

$2K + 1$ times we have that

$$\prod_{k=n-K}^{n+K} \left(1 + I_p \frac{\Delta P_k(\theta)}{I_b \Delta\alpha}\right)^{z_k} = \sum_{p=0}^{\sigma_K} \gamma_p(\theta) \left(\frac{I_p}{I_b}\right)^p$$

where

$$\begin{aligned} \gamma_p(\theta) &= \sum_{r=\max(0, p-z_{n+1})}^{\min(\sum_{n-K}^n z_j, p)} \beta_r(\theta) \binom{z_{n+1}}{p-r} \left(\frac{\Delta P_{n+1}(\theta)}{\Delta\alpha}\right)^{p-r}; \\ \beta_r(\theta) &= \sum_{l=\max(0, r-z_n-z_{n+1})}^{\min(z_{n-K}+z_{n-K+1}, r)} \alpha_l(\theta, n, n+1) \alpha_{p-l}(\theta, n+2, n+3) \\ \alpha_l(\theta, i, j) &= \sum_{m=\max(0, l-z_j)}^{\min(z_i, l)} \binom{z_i}{m} \binom{z_j}{l-m} \left(\frac{\Delta P_i(\theta)}{\Delta\alpha}\right)^m \left(\frac{\Delta P_j(\theta)}{\Delta\alpha}\right)^{l-m} \end{aligned}$$

so that

$$\begin{aligned} O_{10}^n(I_b) &= \frac{1}{\Delta\alpha \Gamma(\alpha) \beta^\alpha} \int_{\zeta_n}^{\zeta_{n+1}} d\theta \int_0^\infty dI_p I_p^{\alpha-1} \exp\left(-\frac{I_p}{\beta'}\right) \sum_p \gamma_p(\theta) \left(\frac{I_p}{I_b}\right)^p \\ &= \frac{1}{\Delta\alpha \Gamma(\alpha) \beta^\alpha} \sum_p \frac{1}{I_b^p} \int_{\zeta_n}^{\zeta_{n+1}} \gamma_p(\theta) d\theta \int_0^\infty dI_p I_p^{p+\alpha-1} \exp\left(-\frac{I_p}{\beta'}\right) \\ &= \frac{1}{\Delta\alpha \Gamma(\alpha) \beta^\alpha} \sum_p \frac{1}{I_b^p} \int_{\zeta_n}^{\zeta_{n+1}} \gamma_p(\theta) d\theta \Gamma(\alpha + p) \beta'^{\alpha+p} \end{aligned}$$

so

$$O_{10}^n(I_b) = \frac{1}{\Delta\alpha} \sum_p \frac{\Gamma(\alpha+p)}{\Gamma(\alpha)} \left(\frac{1}{1 + \tau\Delta P \beta} \right)^{\alpha+p} \left(\frac{\beta}{I_b} \right)^p \int_0^{\Delta\alpha} \gamma_p(\theta) d\theta.$$

Remark. Note that the computation of $\int_0^{\Delta\alpha} \gamma_p(\theta) d\theta$, that may look very time-consuming, can be done before any data are collected. To be computed, only the sums (depending on z_i) have to be computed online.

A.4. When \mathbf{I}_b is uncertain

We now have to apply the marginalization law for both sides.

$$\begin{aligned} L_0 &= \int_0^\infty p(I_b) L_0(I_b) dI_b \\ &= \frac{(\tau\Delta\alpha)^{\sigma_K}}{\Gamma(a) b^a \pi_K} \int_0^\infty I_b^{\sigma_K+a-1} \exp\left(-\frac{I_b}{b'}\right) dI_b \\ &= \frac{(\tau\Delta\alpha)^{\sigma_K}}{\pi_K} \frac{\Gamma(a') b'^{a'}}{\Gamma(a) b^a} \\ &= \frac{(\tau\Delta\alpha)^{\sigma_K}}{\pi_K} \frac{\Gamma(a + \sigma_K)}{\Gamma(a)} \frac{b'^{a'}}{b^a} \end{aligned}$$

where

$$a' = \sigma_K + a; \frac{1}{b'} = \frac{1}{b} + \tau\Delta S$$

Compute now L_1

$$\begin{aligned} L_1 &= \int_0^\infty p(I_b) L_1(I_b) dI_b \\ &= \frac{1}{\pi_K} \frac{1}{\Gamma(a) b^a} \int_0^\infty I_b^{a-1} \exp\left(-\frac{I_b}{b}\right) \frac{1}{\Delta\alpha \Gamma(\alpha) \beta^\alpha} \sum_p \frac{\Gamma(\alpha+p) \beta'^{\alpha+p}}{I_b^p} \\ &\quad \int_{\zeta_n}^{\zeta_{n+1}} \gamma_p(\theta) d\theta (I_b \tau \Delta\alpha)^{\sigma_K} \exp(-I_b \tau \Delta S) dI_b \\ &= \frac{1}{\pi_K} \frac{1}{\Gamma(a) b^a} \frac{(\tau\Delta\alpha)^{\sigma_K}}{\Delta\alpha \Gamma(\alpha) \beta^\alpha} \\ &\quad \sum_p \Gamma(\alpha+p) \beta'^{\alpha+p} \int_{\zeta_n}^{\zeta_{n+1}} \gamma_p(\theta) d\theta \int_0^\infty \exp\left(-\frac{I_b}{b'}\right) I_b^{a''-1} dI_b \\ &= \frac{1}{\pi_K} \frac{1}{\Gamma(a) b^a} \frac{(\tau\Delta\alpha)^{\sigma_K}}{\Delta\alpha \Gamma(\alpha) \beta^\alpha} \sum_p \int_{\zeta_n}^{\zeta_{n+1}} \gamma_p(\theta) d\theta \Gamma(\alpha+p) \beta'^{\alpha+p} b'^{a''} \Gamma(a'') \end{aligned}$$

where

$$a'' = \sigma_K + a - p = a' - p;$$

so

$$O_{10}^n = \frac{1}{\Delta\alpha} \left(\frac{1}{1 + \tau\beta\Delta P} \right)^\alpha \sum_p \left(\frac{\beta'}{b'} \right)^p \frac{\Gamma(\alpha + p)}{\Gamma(\alpha)} \frac{\Gamma(\sigma_K - p)}{\Gamma(\sigma_K + a)} \int_{\zeta_n}^{\zeta_{n+1}} \gamma_p(\theta) d\theta$$